# DRAFT: MODELING AND ANALYSIS OF A MULTI DEGREE OF FREEDOM POINT ABSORBER WAVE ENERGY CONVERTER

**Andrew F. Davis**
Department of Mechanical Engineering
University of Washington
Seattle, Washington 98195
Email: afdavis@uw.edu

**Jim Thomson**
Applied Physics Laboratory
University of Washington
Seattle, Washington, 98195
Email: jthomson@apl.washington.edu

**Tim R. Mundon**
Oscilla Power Inc.
Seattle, Washington, 98103
Email: mundon@oscillapower.com

**Brian C. Fabien**
Department of Mechanical Engineering
University of Washington
Seattle, Washington, 98195
Email: fabien@uw.edu

## ABSTRACT

*This paper illustrates an approach to the modeling of a point absorbing Wave Energy Converter (WEC) with the intent of analyzing the sensitivity of system components. Using first principles, the nonlinear equations of motion were formed to describe the heave motion of a 3 body system. A linearized model was then developed and used to simulate the system in both the time and frequency domains. The input to the model is a time series displacement and a time series velocity that describes the incident waves. A sensitivity analysis is then performed on the system parameters to show how the characteristics of the heave plate, the component masses, and the mass of the entrained fluid affect the performance of the system. The model validation was performed by numerically modeling the Oscilla Power's, Inc. generation 1 device against experimental data from a field test on Lake Washington. The WEC is designed to provide tension along a series of tethers with connected PTO units. The wave input is specified using frequency spectra measured with a nearby Datawell Waverider MK III buoy during the field testing, from which time domain waves are reconstructed.*

## INTRODUCTION

Wave energy has strong potential for being a component of the solution to the problems presented by an increasing energy demand. While the idea of harvesting energy from waves is not new, there has been increasing research in this area. Wave energy converters (WECs) have significant potential in the marine renewable energy field, and pre-commercial prototypes of marine energy devices are being developed and implemented in test situations [1]. However, significant research is still required to develop wave energy into a feasible renewable energy source for coastal regions.

The mooring and installation of a wave energy converter is a significant factor in the cost of produced energy. In shallow waters (i.e., depth less than 30 meters) it may be cost effective to use a rigid foundation, such as a monopile or jacketed pile. However at greater depths or when the wave energy converter must respond dynamically to the water surface (as in the case of point absorber wave energy converters), compliant moorings are necessary. Work has been done model the dynamics of compliant and even slack mooring lines [2]. However, this must be combined with an effective model of WEC dynamics and power

generation is needed in order to optimize the configuration of the mooring lines to minimize the cost of power.

There are several existing commercial software packages such as OrcaFlex, ProteusDS, ANSYS Aqwa, and WAMIT to model the dynamics of marine systems. However, by extending a first principles model to arrays of WECs it will be possible to create generic design tools to maximize the performance of marine energy converters. To better understand the performance of the system and thereby work towards the eventual goal of performance maximization, the final outcome of the system modeling and identification is the parameter sensitivity analysis.

Section 1 presents a general description and the simplifying assumptions that were used to formulate the equations of motion. Section 2 will give a brief description of the deployment of the prototype WEC along with the experimental resources used for validation. In section 3 the numerical methods used to solve for the dynamics of the WEC are shown, then the simulated output and the experimental data is compared. Section 4 develops conclusions on which parameters have the most effect on the efficiency of the system. The study is concluded with a discussion of results in section 5. Finally, the directions of future study are presented in section 6.

## 1 SYSTEM MODEL

The Oscilla WEC is a point absorbing wave energy converter that produces power from the rate of change of tension in the power take off (PTO) units. The simplified model presented assumes that the deflection in the PTOs and the load cell is negligible compared to the deflection in the rope. Because the mooring lines are placed symmetrically, and are not exerting significant tension, this initial model does not include the mooring lines. Considering the vertical motion of the buoy while neglecting the force component of the mooring lines can still produce a reasonably accurate simulation [3].

Figure 1 shows a simplified model of the prototype point absorber. The buoy and components will follow the motion of the wave and the heave plate will create a significant amount of tension in the PTO units. The mass of the heave plate, as it is submerged some distance below the surface, is subject to a greatly reduced wave forcing and its drag and inertia are large enough so that there will always be tension in the central cable. By continuously maintaining tension in the cable, destructive shock loading is avoided during deployment.

## 1.1 EQUATIONS OF MOTION

A simplified model of a mass-spring-damper system is created to represent the system shown in Fig. 1. Figure 2 shows how the WEC is modeled as 3 separate masses with the connections between each mass acting as springs. The primary source of damping in the system is the fluid drag of the masses passing
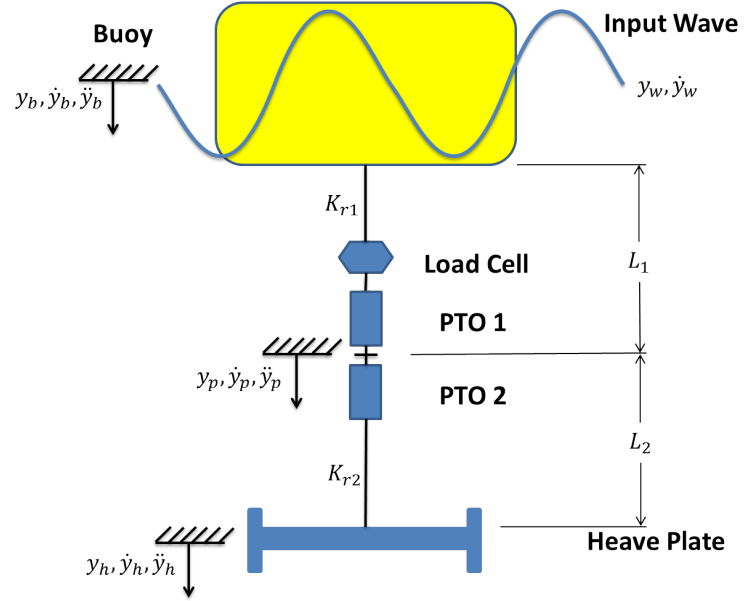


**FIGURE 1**. Simplified model of the Oscilla Power prototype wave energy converter, component displacements are shown from the natural length of each connection and $L_2 >> L_1$. Figure shows three lumped mass components: the displacements $y_b$, $y_p$, and $y_h$ show the positive direction of motion for the buoy, PTO units, and heave plate respectively.

through the water. The dynamics of the WEC are decomposed and analyzed in a similar manner to Refs. [4, 5]. By lumping the load cell and both PTO units together as a single mass the number of equations of motion is reduced from 5 to 3 with little loss of detail. The PTO lumped mass is a reasonable approximation because the load cell and PTO units are connected with rigid links with no appreciable strain. Therefore, the displacements of the 3 smaller components will all be the same as the lumped displacement $y_p$.

Using Newton's law to describe the equation of motion for each mass results in 3 second order ordinary differential equations. The equation of motion for each of the three masses will take the form:

$$m\ddot{y} = F_{Weight} + F_{Buoyancy} + F_{Drag} + F_{Spring}$$

where the dot notation shows the number of time derivatives of a variable and the product of the mass and acceleration is equal to the sum of the forces acting on the mass.

The buoyancy, $B$, and weight of each mass are included in the summation of forces according to the direction conventions established in Fig. 1. It is important to note that the buoy will have a variable buoyant force, whereas the other components will have a constant buoyant force. As more of the buoy becomes
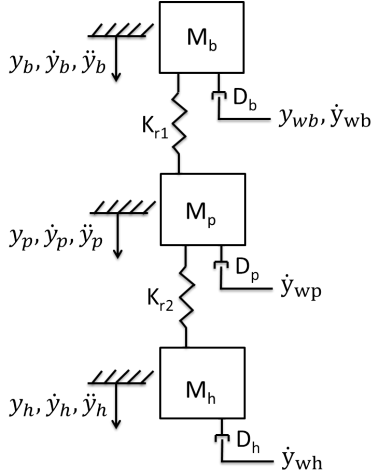
**FIGURE 2**. Mass-Spring-Damper model of the Oscilla Power proto-type.

submerged the weight of the displaced fluid will increase which causes the buoyant force to increase. To compute the force exerted by the buoy the difference between the displacement of the buoy and the surface of the water is multiplied by a term $B_b$, which is in terms of force per unit length.

The drag force is comprised of two main components, the profile drag and the friction drag. The drag force acting on a mass passing through a fluid is computed using the equation:

$$F_{Drag} = \frac{1}{2} C_{drag} A \rho V |V| \qquad (1)$$

where $C_{drag}$ is the coefficient of drag, the computed area, $A$, is the area relevant to the type of drag, $V$ is the net velocity of the object with respect to the fluid particles surrounding it, and $\rho$ is the density of the fluid. The friction drag, $C_f$, is computed by:

$$Re = A^2 \frac{\omega}{\nu} \qquad (2)$$

$$C_f = \frac{0.032}{Re^{1/7}} \qquad (3)$$

where $Re$ is the Reynolds number computed in wave conditions, $A$ is the peak to peak amplitude of the wave, $\omega$ is the frequency, and $\nu$ is the kinematic viscosity of the water [6]. Equation 3 computes the average shear stress coefficient which is used as the coefficient of skin friction. Small amounts of friction will be generated by the boundary layer effects as the water travels along the sides of the masses. The profile drag is the most significant damping component. Dimensionless drag coefficients, $C_d$, are given using the shape and the dimension ratios of the components. The area used to compute the profile drag is the projected

area in the direction of motion.

For this model the spring force $F_{Spring}$ is given as a linear spring constant, $K_{r1}$ and $K_{r2}$, multiplied by the strain from the ropes natural length to compute the spring force acting on each mass. The spring constant $K_{r2}$ is given by the vendor estimation of the rope used and $K_{r1}$ is large enough to ensure that the buoy and the PTO mass move together. Since the displacements are measured from an equilibrium position rather than from a single reference point, the strain is computed by finding the difference of the displacements.

Three separate equations of motion are formed to describe the independent motion of all three lumped masses. The Oscilla system has a significantly more rigid connection between the buoy and the PTO units than the connection between the PTO units and the heave plate. This is reflected in the model by the use of the two different spring constants $K_{r1}$ and $K_{r2}$. Nevertheless, three equations of motion are modeled because it is the goal of this research to evaluate how variations in the structural properties effect the power production of the system. The resulting 3 differential equations are:

$$m_b \ddot{y}_b = m_b g - B_b (y_b - y_w)$$
$$- \frac{C_{Db}}{2} A_b \rho (\dot{y}_b - \dot{y}_w e^{-\frac{1}{2}k}) |\dot{y}_b - \dot{y}_w e^{-\frac{1}{2}k}| \qquad (4)$$
$$- \frac{C_f}{2} A_{bwet} \rho (\dot{y}_b - \dot{y}_w e^{-\frac{1}{2}k}) |\dot{y}_b - \dot{y}_w e^{-\frac{1}{2}k}|$$
$$- K_{r1} (y_b - y_p)$$

$$m_{vp} \ddot{y}_p = m_p g - B_p$$
$$- \frac{C_{Dp}}{2} A_p \rho (\dot{y}_p - \dot{y}_w e^{-7k}) |\dot{y}_p - \dot{y}_w e^{-7k}| \qquad (5)$$
$$- \frac{C_f}{2} A_{pwet} \rho (\dot{y}_p - \dot{y}_w e^{-7k}) |\dot{y}_p - \dot{y}_w e^{-7k}|$$
$$- K_{r1} (y_p - y_b) - K_{r2} (y_p - y_h)$$

$$m_{vh} \ddot{y}_h = m_h g - B_h$$
$$- \frac{C_{Dh}}{2} A_h \rho (\dot{y}_h - \dot{y}_w e^{-14k}) |\dot{y}_h - \dot{y}_w e^{-14k}| \qquad (6)$$
$$- \frac{C_f}{2} A_{hwet} \rho (\dot{y}_h - \dot{y}_w e^{-14k}) |\dot{y}_h - \dot{y}_w e^{-14k}|$$
$$- K_{r2} (y_h - y_b)$$

It is important to note two features of the equations of motion, the virtual mass denoted with the $m_v$ and the exponential attenuation terms. The virtual mass for each component is the sum, $m_v = m + m_a$, where $m_a$ is the added mass correction factor and $m$ is the mass. The added mass term is used to compensate for the fluid that is carried along with each mass as the components pass through the water. This entrained fluid may be a substantial modification to the inertia of each component, however it is important to note that this added mass does not contribute the weight of the components.

3

When computing the added mass in the heave direction the geometry of the masses is required, and with this information an expression for the hydrodynamic mass per unit length is given. The numerical model is simulated assuming that there is no added mass for the buoy. In the sensitivity study the effect of a nonzero added mass for the buoy is shown. Typically a tool such as WAMIT is used to determine added mass coefficients, however for the purpose of this study a simplified approximation for objects under the effect of surface waves is used to calculate the added mass. Computing the added mass for the PTO units and the heave plate shows that the added mass can greatly vary based on the geometry, as a result no single expression can compute the added mass for all objects. The added mass of the PTO units was roughly 4% of the actual mass and the added mass of the heave plate was 40% of the mass. The hydrodynamic mass of the vertical motion of a circular disk which represents the heave plate is given by the expression $m_h = 8/3\rho a^2$, where $\rho$ is the density and $a$ is the radius of the disk. The added mass of the PTO units is computed in a similar manner to the added mass of the heave plate [7].

The second important feature of the equation is the exponential terms that modify the wave velocity $\dot{y}_w$. The attenuation terms result from the linear deep water wave theory that describes a fluid velocity that is maximum at the surface of the water and decreases rapidly with depth. An attenuation term is used to describe the water particle velocity surrounding each mass. This is given by $e^{-depth*k}$, where $k = \frac{\omega^2}{g}$ is the wave number. The wave number is an expression of the wave frequency, $\omega$, and the gravitational acceleration, $g$. The wave period that was used to compute the wave frequency is 3 seconds. While 3 seconds is a very small wave period for ocean it is reasonable for a wave period in Lake Washington. The exponential attenuation term computes a very small velocity at the depth of the PTO units and by extension the wave velocity at the depth of the heave plate is negligible during operational conditions.

## 1.2 SPECTRAL METHOD

The nonlinear damping coefficient is composed of the profile drag and the skin friction.

$$C = \frac{1}{2}C_D A_{body}\rho + \frac{1}{2}C_f A_{wet}\rho \tag{7}$$

$A_{wet}$ is assumed to be half the surface area of the buoy to obtain a linear damping. The wetted areas of the other bodies are calculated based on geometry. By [8] the nonlinear damping can be approximated by:

$$F_{damping} = C\dot{x}|\dot{x}| \tag{8}$$
$$= CA_o\omega_o|\dot{x}| \tag{9}$$

where, $A_o$ and $\omega_o$ are the peak to peak amplitude and the wave frequency respectively. This allows the linear damping term to be written Eqn. (10). Damping coefficients are often a very uncertain component of a model, as such a small period of 1.7 seconds is used to guarantee that the damping is not underestimated throughout the full range of the velocity. An over estimation of the simplified damping term at this point in the model is acceptable considering that there are additional forms of damping, such as radiation damping, that would cause additional losses in a real system.

$$D = \frac{1}{2}\left[C_D A_{body} + C_f A_{wet}\right] \tag{10}$$

The damping force is modeled by $F_{damping} = D\dot{x}$. The input function as $y_w = A\sin(\omega t)$ and $\dot{y}_w = A\omega\cos(\omega t)$. The terms are separated and organized for state space formulation.

$$m_b\ddot{y}_b = -D_b\dot{y}_b - B_b y_b - K_{r1}y_b + K_{r1}y_p + m_b g + B_p y_w$$
$$+ D_b\dot{y}_w e^{-\frac{1}{2}k} \tag{11}$$
$$m_{vb}\ddot{y}_p = -D_p\dot{y}_p - K_{r1}y_p - K_{r2}y_p + K_{r1}y_b + K_{r2}y_h$$
$$+ m_p g - B_p + D_p\dot{y}_w e^{-7k} \tag{12}$$
$$m_{vh}\ddot{y}_h = -D_h\dot{y}_h - K_{r2}y_h + K_{r2}y_p + m_h g - B_h + D_h\dot{y}_w e^{-14k} \tag{13}$$

With a 3 degree of freedom system we will now create the standard state space formulation with the wave input.

$$M\ddot{y} = Ky + C\dot{y} + e_o + e_1 y_w + e_2 \dot{y}_w$$

$$M = \begin{bmatrix} m_b & 0 & 0 \\ 0 & m_p + A_p & 0 \\ 0 & 0 & m_h + A_h \end{bmatrix}$$

$$K = \begin{bmatrix} -(B_b + K_{r1}) & K_{r1} & 0 \\ K_{r1} & -K_{r1} - K_{r2} & K_{r2} \\ 0 & K_{r2} & -K_{r2} \end{bmatrix}$$

$$C = \begin{bmatrix} -D_b & 0 & 0 \\ 0 & -D_p & 0 \\ 0 & 0 & -D_h \end{bmatrix}$$

$$e_o = \begin{bmatrix} m_b g \\ m_p g - B_p \\ m_h g - B_h \end{bmatrix} \quad e_1 = \begin{bmatrix} B_b \\ 0 \\ 0 \end{bmatrix} \quad e_2 = \begin{bmatrix} D_b e^{-\frac{1}{2}k} \\ D_p e^{-7k} \\ D_h e^{-14k} \end{bmatrix}$$

Let $q_1 = y$ and $q_2 = \dot{y}$ to perform the reduction of order. The new first order system is written in matrix form as follows.

$$\dot{q}_1 = q_2 \tag{14}$$
$$\dot{q}_2 = M^{-1}\left[Kq_1 + Cq_2 + e_o + e_1 y_w + e_2 \dot{y}_w\right] \tag{15}$$

With $q = \begin{bmatrix} q_1 \\ q_2 \end{bmatrix}$ while $y_w$ and $\dot{y}_w$ are unchanged. The new matrix form is indicated by the hat notation.

$$\dot{q} = \hat{A}q + \hat{B}_o + \hat{B}_1 y_w + \hat{B}_2 \dot{y}_w \qquad (16)$$

$$\hat{A} = \begin{bmatrix} 0 & I \\ M^{-1}K & M^{-1}C \end{bmatrix} \hat{B}_o = \begin{bmatrix} zeros(3,1) \\ M^{-1}e_o \end{bmatrix}$$

$$\hat{B}_1 = \begin{bmatrix} zeros(3,1) \\ M^{-1}e_1 \end{bmatrix} \hat{B}_2 = \begin{bmatrix} zeros(3,1) \\ M^{-1}e_2 \end{bmatrix} q = \begin{bmatrix} y_b \\ y_p \\ y_h \\ \dot{y}_b \\ \dot{y}_p \\ \dot{y}_h \end{bmatrix}$$

Next apply the Laplace transform with zero initial conditions. When considering the system from a steady state position the buoy is at the equilibrium position and then the wave forcing function is applied, this allows the buoyancy and weight terms, comprising $\hat{B}_o$, to be ignored. The transfer function $\frac{Q}{Y_w}$ is formed by algebraic manipulation of Eqn. (17), and is useful to determine the input-output relationship of the motion of the WEC components.

$$(sI - \hat{A})Q = (\hat{B}_1 + \hat{B}_2 s)Y_w \qquad (17)$$

$$\frac{Q}{Y_w} = (sI - \hat{A})^{-1}(\hat{B}_1 + \hat{B}_2 s) \qquad (18)$$

The symbolic computation is done using the MATLAB symbolic toolbox. This transfer function is defined in the frequency domain by multiplying the displacement transfer function by the derivative operator squared and is essentially defined as a transfer function with displacement input and acceleration output. Here, A is the acceleration of the system and $Y_w$ is the previously defined wave input.

$$\frac{A}{Y_w} = s^2 \frac{Q}{Y_w} \qquad (19)$$

The frequency response of the linear system provides added certainty in the solution, by verifying that the acceleration transfer function behaves in the expected manner. Reference [9] provides detailed description of the linear interactions of oscillating systems.

## 2 DEPLOYMENT

The Oscilla WEC first generation prototype was deployed in Lake Washington, by the University of Washington Applied Physics Laboratory. During this 3 month deployment, data was collected for the 3 axis accelerations of the buoy enabling the fundamental means of validating the numerical model of the WEC. Additionally, a load cell in series with the PTO units measures the tension between the PTOs and the buoy. Figure 2 shows a short time span of the raw data collected during the Lake Washington deployment.

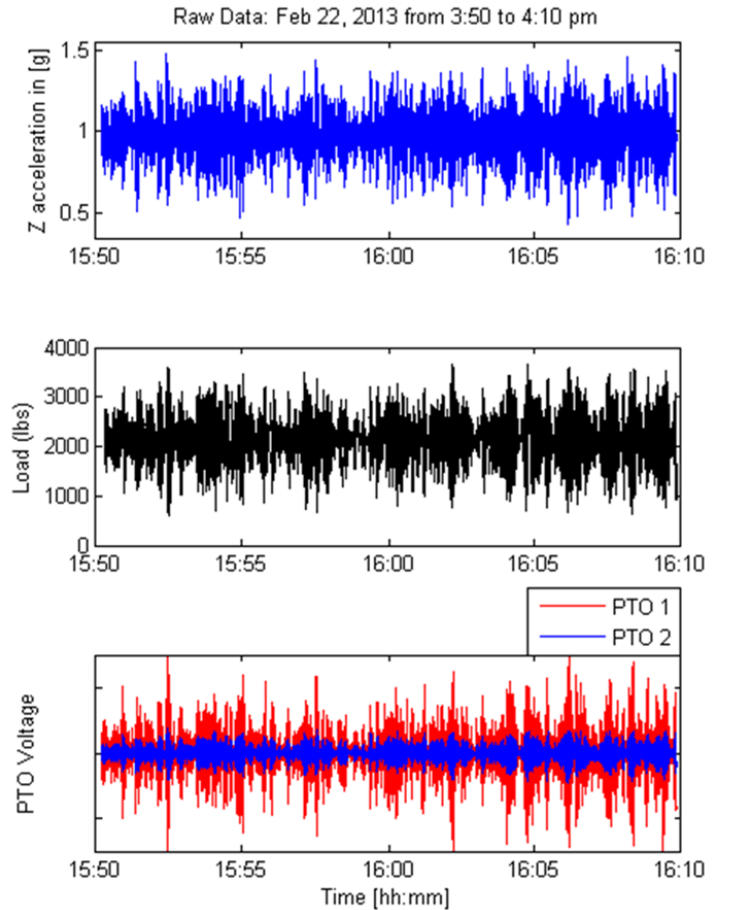Lake Washington was a safe testing environment with its



**FIGURE 3**. Sample raw data from the oscilla power wave energy converter generation 1 deployment in Lake Washington, this data takes place in a winter storm to show well defined wave characteristics.

relatively calm waters for the vast majority of the time, however during occasional storms the 5 kilometer fetch and increased wind speed allow for more fully developed wave conditions. Incident wave data was taken using a Waverider MK III directional buoy for the duration of the Oscilla Power deployment. Internal to the Waverider buoy, data is processed and stored as a Power Spectral Density (PSD). It was therefore necessary to convert the

5

Waverider PSD data to an amplitude spectrum by multiplying by the bandwidth, then dividing the square root by half to provide valid one-sided amplitude inputs to the simulation used to validate the response of the linear model.

The Pierson-Moskowitz (PM) spectrum was used to model the wave data as a continuous function of frequency. The Pierson-Moskowitz spectrum is a 1 parameter spectrum based on the wind speed in meters per second at 19.5 meters above the steady water line [10]. The PM spectrum is characterized by the assumption that the waves are generated by a steady wind with a very long fetch,

$$E(f) = \frac{0.0081 * g^2}{(2 * \pi)^4 f^5} e^{\left(-0.74 \left(\frac{2 * \pi * U_w * f}{g}\right)^{-4}\right)} \qquad (20)$$

where E is the expected spectral amplitude at a given frequency, g is the acceleration due to gravity, 0.0081 is the Phillips constant, f is frequency given in Hz and $U_w$ is the wind velocity in meters per second at an elevation of 19.5 meters.

In order to determine the wind speed, an optimization function was used to find the wind speed that minimized the error between the PM and the Waverider Spectra. Fig 4. shows two examples of the best fit PM spectra. While the high peaks in the Waverider data are not captured by the continuous function, the realistic higher frequencies are included. It is important to note that using a JONSWAP spectrum would add an extra parameter providing a more accurate model for fetch limited conditions [10]. However, the experimental conditions are well represented with the more simple PM spectrum.

## 3  NUMERICAL SIMULATION

After the model of the WEC was formulated, a time domain simulation program was implemented in MATLAB to simulate the heave motion of the WEC when subjected to a spectral wave input. The time domain simulation requires time series data for both the displacement and the velocity of the input wave. Since this system involves stiff differential equations a small time step and a stiff ODE solver is used to simulate the motion of the 3 bodies of the WEC. The acceleration was then computed from the simulated displacements and velocities, and the acceleration amplitude spectrum was computed using a Discrete Fourier Transform.

By using a transfer function, it is possible to compute the acceleration amplitude spectrum given a wave input defined by the PM spectrum by Eqn. (20). This can be compared to the amplitude spectrum of acceleration provided by applying a Discrete Fourier Transform to the vertical acceleration data in Fig. 2. The spectral methods provided excellent validation of the numerical integration of the time series solution. However, Fig. 5 shows the power spectral density (PSD), which was generated using the
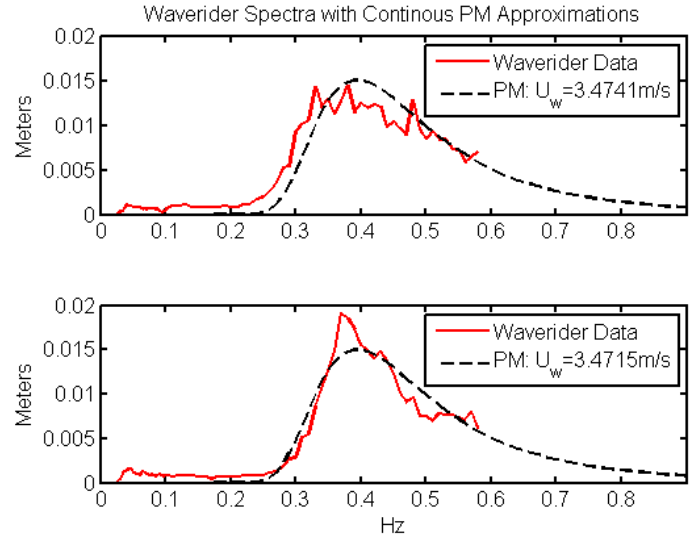


**FIGURE 4**. Pierson-Moskowitz approximations of incident wave data, wind velocity is determined by minimizing the error between wave data and function approximation.

time domain simulation, of the acceleration of the buoy for both deployment data and the numerical model for accuracy and clarity of comparison.

The dynamics of the WEC are verified using the amplitude spectrum of the acceleration measured in the buoy of the Oscilla WEC. The model prediction of the acceleration response captures the experimental acceleration response in the frequency range from 0.3 Hz to 1 Hz. Figure 5 shows that the dynamics of the converter is well represented by the model. Once the response of the model was verified against the experimental results, the time domain simulation used to estimate the power output of the model.

### 3.1  TIME DOMAIN SIMULATION

The time domain simulation of the WEC in response to a wave input was computed by using a numerical integrator in MATLAB. The PM spectrum of wave amplitudes was used to generate the wave input to the time domain model. Although real waves do not have a true random phase, the time domain input was created by randomizing the phase for each frequency and amplitude pair. The velocity input to the model was generated by the time derivative of the displacement input.

Figure 6 shows the relative position from static equilibrium, illustrating the relative displacement of all three bodies of the WEC compared to the wave input. This enables good visualization of how the converter is moving when being forced by the incident input. As expected relative positions of the components
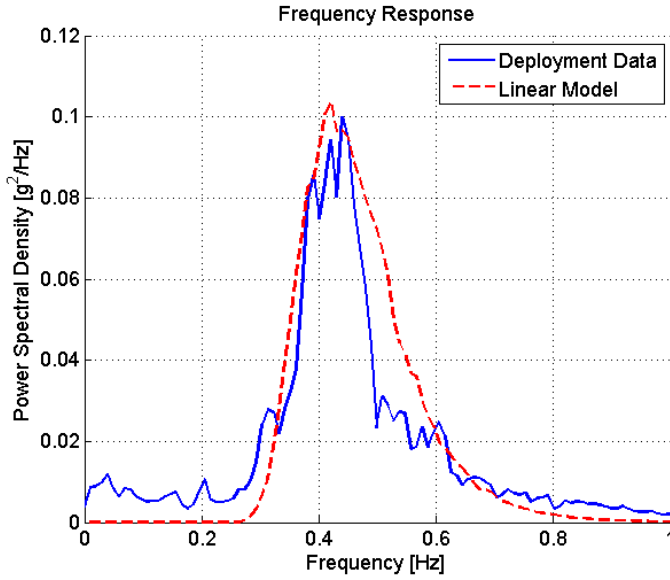
**FIGURE 5**. Power spectral density of the experimental data and the linear model. The measured acceleration, $\ddot{y}_b$ is the acceleration experienced by the buoy.



**FIGURE 6**. Time domain simulation of the relative deflections of the 3 bodies with reference to the wave input, displacement direction is opposite of the convention established in Figs. 1 & 2 for ease of visualization

**TABLE 1**. Error in the modeled power, Feb. 22, 2013 to Feb. 23, 2013

| Time | $T_D$ [s] | $H_s$ [m] | % Error |
|---|---|---|---|
| 22:30-23:00 | 2.56 | 0.14 | $-3.6$ |
| 23:00-23:30 | 2.53 | 0.14 | 8.0 |
| 23:30-24:00 | 2.58 | 0.21 | 7.9 |
| 00:00-00:30 | 2.67 | 0.21 | $-9.1$ |
| 00:30-01:00 | 2.67 | 0.28 | $-11.0$ |
| 01:00-01:30 | 2.63 | 0.28 | 3.1 |
| 01:30-02:00 | 2.54 | 0.25 | 13.5 |

show that there is never a situation where the rope, holding the components together, is slack which would cause shock loading on the PTO units.

## 3.2 PREDICTED POWER PRODUCTION

By using the validated model of the motion of the buoy and comparing the predicted PTO output based on the rate of change of tension it is possible to identify the linear proportionality constant $\alpha$ relating the tension derivative to the power production $\mathbb{P} = \alpha \dot{T}$. Here, $\mathbb{P}$ is the power production of the PTO units and $\dot{T}$ is the time rate of change of the tension in the PTO units. Oscilla Power has developed models describing the power production of the magnetostriction based power take off units which are able to production energy from the entire spectrum of the wave input [11].

After identifying the proportionality constant the model is compared against other data sets during the same storm. For reasons of propriety Tab. 2 only shows the error associated with the predicted power.

Table 1 shows the error between the power production from the WEC and the predicted power production from the time domain model. $T_D$ is the dominant period and $H_s$ is the significant wave height of the input. From this table it is shown that the time domain model has reasonable certainty given the simplified nature of the wave model. The assumption of a purely random phase also adds a small amount of uncertainty when determining
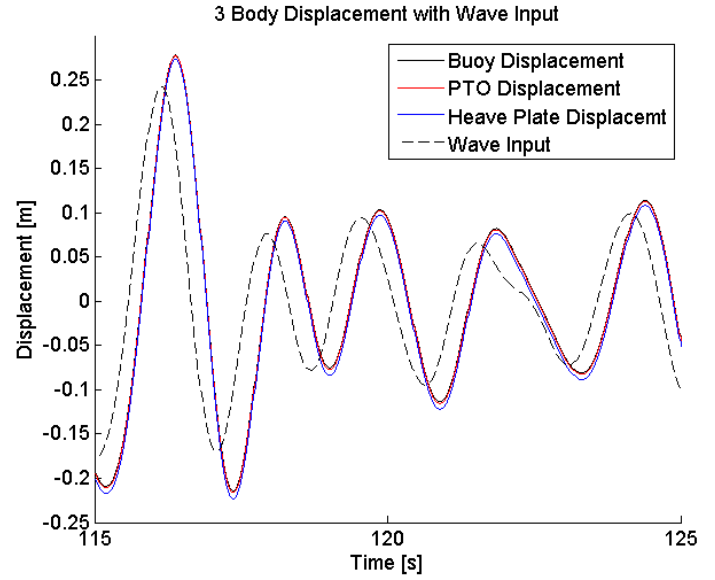
the coefficient to predict the power generation of the system.

## 4 SENSITIVITY ANALYSIS

By using a reference data set it is possible to perform a sensitivity analysis by changing parameters and computing the new power production. The analysis is performed in two stages, first varying each adjustable parameter by positive 5% and then posi-

**TABLE 2**. Proportional power change: $\%\Delta\mathbb{P}_1$ is the change in power production when the parameter is changed by +5%, $\%\Delta\mathbb{P}_2$ is the change in power production when the parameter is changed by +20%

| Parameter | Initial Value | $\%\Delta\mathbb{P}_1$ | $\%\Delta\mathbb{P}_2$ |
|---|---|---|---|
| Buoy mass | 570kg | 0.0% | -0.2% |
| PTO mass | 260kg | 1.2% | 4.3% |
| Heave Plate mass | 705kg | 2.5% | 9.3% |
| Buoy added mass | 0kg | 0.8% | -0.8% |
| PTO added mass | 4% mass | 0.2% | 0.2% |
| HP added mass | 40% mass | 1.0% | 3.4% |
| Spring: $K_{r1}$ | 1,250,000 $\frac{N}{m}$ | -0.1% | 0.3% |
| Spring: $K_{r2}$ | 270,000 $\frac{N}{m}$ | 0.7% | 0.3% |
| Buoy buoyancy | 22,260$\frac{N}{m}$ | 2.5% | 10.0% |
| PTO buoyancy | 700N | 1.1% | 0.0% |
| HP buoyancy | 1000N | 0.1% | 0.2% |
| Buoy drag, $D_b$ | coefficient=1.7 | -1.5% | -6.5% |
| PTO drag, $D_p$ | coefficient=0.87 | 0.1% | 0.3% |
| HP drag, $D_h$ | coefficient=1.7 | 0.2% | -0.3% |

tive 20%.

Table 2 shows the parameters that are varied in the sensitivity analysis along with the correspond values used in the simulation. It can be seen that the greatest effect on the power production is the mass of the heave plate and the buoyancy of the buoy. This implies that the system is dominated by the inertia of the components and entrained fluid rather than the drag, as may be expected. Despite the great effect the buoyancy of the buoy has on the power production it may be that a disproportionately large buoy is not plausible. The heave plate parameters also have significant impact on the performance of the WEC. Tab. 2 shows that by increasing the mass of the heave plate or by increasing the mass of the fluid entrained by the heave plate the total power production will be increased.

Since the simulation was performed with zero added mass initially, the sensitivity analysis used a reasonable range of added mass coefficients based on the added mass of a similarly shaped object. The first power production change was estimated by assuming an added mass that was 20% of the original buoy mass, and the second power production change was computed using an added mass equal to 40% of the original buoy mass. As shown in the table, a significant change in the estimation of the added mass does not produce a significant change in the estimated power production. Likewise, a dramatic increase in both spring constants produced less than a 1% change in the power production.

In the sensitivity analysis it is important to recognize that the power production is not based on the tension that the PTO units are subjected to, but rather the time rate of change of the tension. Careful consideration should be taken when considering the effect that parameters will have on a point absorber WEC with a different power take out.

## 5 CONCLUSION

This paper presented an approach to the modeling and validation of a multiple multiple body point absorber wave energy converter. By forming the equations of motions from first principles rather than using a commercial hydrodynamics package a model is established for the development of control aimed at reducing the cost of producing energy with arrays of wave energy converters. The equations of motion are developed and then linearized with the goal of validating the amplitude spectrum with experimental data.

Simulations are performed using both spectral and time domain methods using MATLAB to validate the amplitude spectrum of the acceleration of the wave energy converter. After determining a model for the wave input based on incident wave data taken during the deployment, a time domain simulation is used to estimate the power production of the system. A linear proportionality constant is used to relate the time rate of change of tension, applied to the power take off units, to the power generated. The model is then used to compare the predictions with the experimental power production for several different time intervals.

Finally, a sensitivity analysis was used to show that this system is dominated by inertia more than drag. As a result, the design of the system should pay careful attention to the mass of each component and the added mass of the entrained fluid. The heave plate is also shown to be an important component for the performance of the system. The fluid drag and the weight of the heave plate must ensure that the PTO units are never in slack conditions, while not producing an adverse effect on the power production as demonstrated in the sensitivity analysis.

## 6 FUTURE WORK

Modeling the dynamics of a multiple degree of freedom system will be the first step to model the moorings of marine energy converter arrays. As the foundation to larger simulations, there will be continued research aimed at decreasing the error between the model and deployed wave energy converter. By expanding the model to include the mooring lines additional sensitivity analysis can be performed to identify the performance characteristics of various methods of station keeping [12].

Point absorber WECs show their greatest potential to deployed in large energy converter farms [13]. With large numbers of WECs in mind it is necessary to model a network of converters to optimize the performance of a marine energy farm while maintaining the survivability of the converters in extreme conditions. As shown in [3], an accurate simulation of the dynamics of multiple degree of freedom wave energy converters is possible using a state space formulation. A mathematical basis for optimizing the configuration of the system will be formed by extending the work done in [14, 15] to validate networked wave energy converters. The validated dynamics of a general WEC can now be used to test controls methods on a wide variety of wave energy converters.

## REFERENCES

[1] Johanning, L., Smith, G., and Wolfram, J., 2006. "Mooring design approach for wave energy converters". *Proceedings of the Institute of Mechanical Engineers, Part M: Journal of Engineering for the Maritime Environment*.

[2] Fabien, B. C., 2012. *Nonlinear Approaches in Engineering Applications*. Springer, ch. Equilibrium of a Submerged Body with Slack Mooring, pp. 211–236.

[3] de Andrés, A., Guanche, R., Armesto, J., del Jesus, F., Vidal, C., and Losada, I., 2013. "Time domain model for a two-body heave converter: Model and applications". *Ocean Engineering*(72), pp. 116–123.

[4] Dewhurst, T. e. a., 2013. "Dynamics of a floating platform mounting a hydrokinetic turbine". *Marine Technology Society Journal,* **47**(4), pp. 45–56.

[5] Wacher, A., and Neilsen, K., 2010. "Mathematical and numerical modeling of the aquabuoy wave energy converter". *Mathematics-in-Industry Case Studies Journal,* **2**, pp. 16–33.

[6] Babanin, A. V., 2006. "On a wave-induced turbulence and a wave mixed upper ocean layer". *Geophysical Research Letters,* **33**.

[7] Brennen, C., 1982. A review of added mass and fluid inertial forces. Tech. rep., Naval Civil Engineering Laboratory.

[8] Chakrabarti, S., and Cotter, D., 1992. "Hydrodynamic coefficients of a moored semisubmersible in waves". *Journal of Offshore Mechanics and Arctic Engineering,* **114**(1), pp. 9–15.

[9] Falnes, J., 2002. *Ocean waves and oscillating systems: linear interactions including wave-energy extraction*. Cambridge University Press, ch. 2-5.

[10] US ARMY CORPS OF ENGINEERS. *Costal Engineering Manual - Part II, Water Wave Mechanics*.

[11] Nair, B. e. a., 2013. "Low-cost utility-scale wave energy enabled by magnetostriction". In Marine Energy Technology Symposium (GMREC), Washington, DC (2013).

[12] Fitzgerald, J., and Bergdahl, L., 2008. "Including moorings in the assesment of a generic offshore wave energy converter: A frequency domain approach". *Marine Structures,* **21**, pp. 23–46.

[13] Falnes, J., and Hals, J., 2011. "Heaving buoys, point absorbers and arrays". *Phil. Trans. R. Soc. A,* **370**, pp. 246–277.

[14] Vicente, P. C., Falcão, A. F. d. O., Gato, L. M., and Justino, P. A. P., 2009. "Dynamics of arrays of floating point-absorber wave energy converters with inter-body and bottom slack-mooring connections". *Applied Ocean Research*, pp. 267–281.

[15] Gao, Z., and Moan, T., 2009. "Mooring system analysis of multiple wave energy converters in a farm configuration". In Proceedings of the European Wave and Tidal Energy Conference.